ELSEVIER

Computers and Electronics in Agriculture
36 (2002) 215–223

Computers and electronics in agriculture

www.elsevier.com/locate/compag

Computer vision based system for apple surface defect detection

Qingzhong Li [a], Maohua Wang [b,*], Weikang Gu [a]

[a] *Department of Information and Electronic Engineering, Zhejiang University, Hangzhou, People's Republic of China*

[b] *Research Centre for Precision Agriculture, China Agricultural University, Beijing, People's Republic of China*

Abstract

A novel automated apple surface defect sorting experimental system based on computer image technology has been developed. The hardware system has the advantage of being able to inspect simultaneously four sides of each apple on the sorting line. The methods, including image background removal, defects segmentation and identification for stem-end and calyx areas, were developed. The results show that the experimental hardware system is practical and feasible, and that the proposed algorithm of defect detection is effective.

Keywords: Machine vision; Apple; Surface defect

1. Introduction

China is a large agricultural country. Its annual apple production is over 17 million tons. Much of the sorting and grading process, however, is still not automated. Hand inspection of fruit is tedious and can cause eye fatigue; it is also subject to sorting errors due to different judgment by different persons. Although some quality inspection procedures such as color, size, and shape are performed by automated systems in western countries, the automation of the defect sorting process is still a challenging subject due to the complexity of the problem. Currently there are two main problems blocking the implementation of automatic apple grading. One is

* Corresponding author
E-mail address: mhw@public.bta.net.cn (M. Wang).

0168-1699/02/$ - see front matter
PII: S0168-1699(02)00093-5

how to acquire the whole surface image of an apple by cameras at an on-line speed. The other is how to quickly identify the stem and calyx. To solve the first problem, Growe and Delwiche (1996), Tao (1996) used a roller conveyer system. The drawback of this method was that the camera above the conveyor cannot inspect the two end sides of the horizontal axes of the rolling fruits. For the second problem, Throop et al. (1997) developed two kinds of orienting devices. These devices were used to rotate apples of different varieties along the stem–calyx axes. But the results showed that the varieties that were successfully oriented with one system would not orient using the other device. Yang (1993) used structured lighting to identify the stem and calyx of apples. The major problem with the structured lighting is the misclassification of laser lines on the image. Wen and Tao (1998) successfully developed a dual-camera NIR/MIR imaging method for apple defect recognition and stem–calyx identification. But the MIR camera is too expensive to use in China.

The objective of the work described in this paper was to develop an experimental system that can inspect four sides of each apple, simultaneously, at on-line throughput (over three to four fruits per s) and the corresponding methods for effective defects segmentation and recognition.

2. System setup overview

A system capable of inspecting four directions of each apple at on-line throughput was developed. The setup of the system is shown in Fig. 1. It consisted of a feeding unit, an apple uniform spacing unit, a machine vision system, and a sorting conveyor. The basic feeding conveyor transported the apples to the uniform spacing conveyor. Then, the apples were fed to the machine vision system for the defect

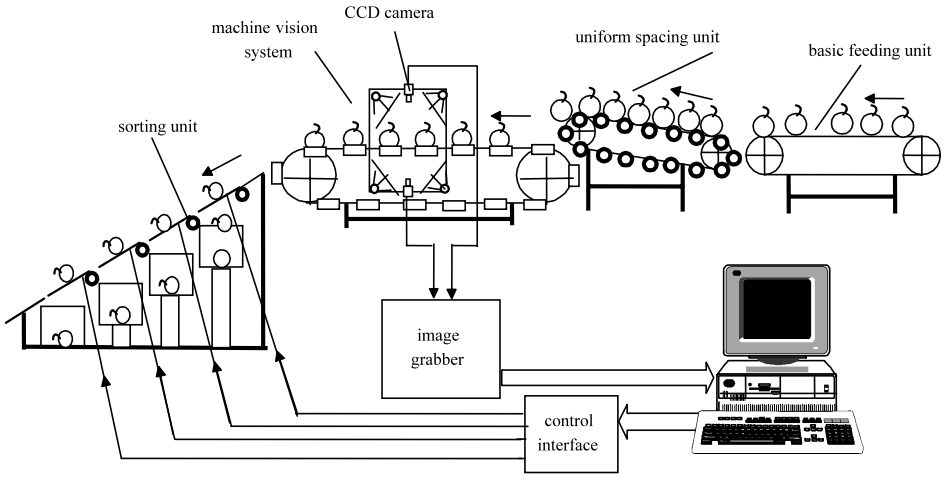

Fig. 1. Schematic representation of apple defects sorting system.

inspection. Finally, the automatic sorting unit accomplished the apple grading operation.

The machine vision system included a cup type conveyor, a lighting chamber for the desired spectrum and light distribution for fruit illumination, two cameras, and an image grabbing card with four input channels inserted in a microcomputer (processor speed: 500 MHz). . As an experimental system, the fruit-feeding system and the automatic sorting system were not constructed in the first stage of the research.

To achieve a basically complete inspection of apples on the fruit sorting line, two identical monochromatic cameras were mounted above and below the conveyor, respectively. The setup of the vision system is shown in Fig. 2. The image sensors in the cameras had an actual resolution of 580 horizontal and 350 vertical TV lines. Each camera was synchronized to another timing source and had a variable electronic shutter. Identical 8.5 mm focal length C-mount lenses were attached to the cameras, with interference band-pass optical filters (840 nm) attached to the outside of each lens. The conveyor was composed of fruit cups without bottoms as shown in Fig. 2. Two mirrors were fixed on both sides of the conveyor; thus the camera above the conveyor took three side views of an apple, i.e. top and two sides. The camera below the conveyor took a bottom view of the fruit. Moreover, this imaging system was able to inspect several apples on the conveyor simultaneously. This scheme had the advantage of being able to inspect simultaneously four sides of each apple while it was traveling on the conveyor.

3. Algorithm description

The algorithm developed for the surface defect detection mainly included modules of image preprocessing, defect segmentation, stem–calyx recognition, and defect area calculation and grading. The algorithm is shown schematically in Fig. 3.

3.1. Image background removal through a method of subtraction

The image backgrounds in the mirror and on the conveyor were different, so it was impossible to segment the parts of fruit by a simple threshold process. Therefore, a subtracting method was used, as depicted below:

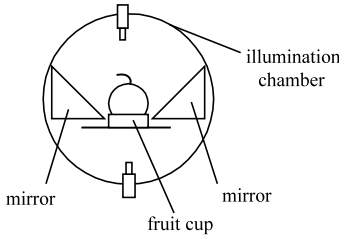

Fig. 2. Setup of vision system.

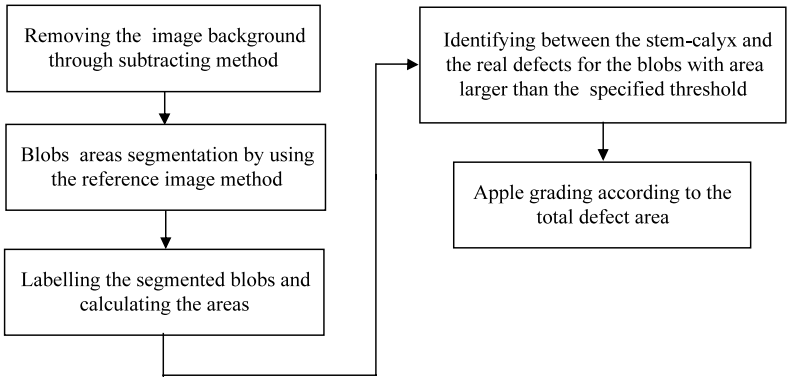

Fig. 3. Flowchart of defect detection algorithm.

$$g(x,\ y) = \begin{cases} 0, & \text{if } |f(x,\ y) - b(x,\ y)| \le T \\ f(x,\ y), & \text{otherwise} \end{cases} \quad (1)$$

where $g(x, y)$ is the image after its background has been removed, $f(x, y)$ is the original image, $b(x, y)$ is the background image, and T is the threshold.

3.2. Defects segmentation by using reference apple images

Apples under inspection had substantially spherical shapes, resulting in curved distributed image intensity. This curved distribution caused the intensity values of the normal surface near the boundary to be lower than the intensity of the defect patches on the surface of the fruit. It is difficult to use any simple global threshold segmentation algorithm for defect extraction. Local adaptive methods could be used for defect segment extraction. However, the processing time prevents their practical use in real-time fruit sorting operations. Based on the reference image of an apple, Li and Wang (1999) developed a method to accomplish defect segmentation for a curved fruit image. In this method, a reference fruit image (RFI) was generated first and the original fruit image for inspection was then normalized to achieve the normalized reference fruit image (NRFI). Finally by subtracting normalized original fruit image (NOFI) from the NRFI and then by simple threshold processing, the defects could be extracted easily.

3.3. Stem–calyx identification based on fractal features and artificial neural network

During the defect inspection process, it is difficult to distinguish the stem and calyx from true defects, because they are similar to defective spots in the image. Based on fractal dimensions and neural networks (NN), the authors of this paper developed a novel method to distinguish the stem–calyx concave area from true defects.

Fractal is a term used to describe the shape and appearance of the objects, which have the properties of self-similarity and scale invariance. Fractal dimension is a scale independent measure of the degree of surface roughness or boundary irregularity. Although the intensity of stem–calyx and true defects are similar, their fractal features may be different. Moreover, fractal analysis in the frequency domain only depends on the frequency distribution of the image surface. These fractal textural features would be independent of the variation of ambient light intensity and orientation of the apples being sorted. So this method is suitable for apple sorting operations where apples are in random orientations. The image distribution can be regarded as a three-dimensional curved surface. Based on the above consideration, five fractal dimensions including one traditional fractal dimension and four oriented fractal dimensions were selected as the features of the image spots produced by stem–calyx concave area or true defects. The four oriented fractal dimensions (D_1, D_2, D_3, D_4) are shown in Fig. 4. In fact, the oriented fractal dimensions were the fractal dimensions of the curves in the corresponding directions (Fig. 5). The five fractal dimensions are calculated by the method derived by Li and Wang (2000). The digital image can be depicted as: $Z = f(x, y)$, where (x, y) is the coordinates of a pixel; Z is the gray value. Assuming the area of the image is M × M the x-y plane of the image is divided into grids with area $\delta \times \delta$. The maximum and the minimum of gray values in the grid are expressed as $u_\delta(i, j)$ and $b_\delta(i,j)$, respectively. And their difference is $d_\delta = u_\delta(i, j) - b_\delta(i,j)$. Then the total nonempty box number (N_δ) for all the $\delta \times \delta$ grids is calculated as:

$$N_\delta = \frac{\sum_{i,j} d_\delta(i, j)}{\delta} \tag{2}$$

For all the given δ a data set from a series of points $\log \delta$, $\log N_\delta$ can be obtained. Through linear regression of the points ($\log \delta$, $\log N_\delta$), the minus slope of the regression line gives the estimated fractal dimension. The four oriented dimensions can be estimated by using a similar method.

A feedforward backpropagation (BP) NN algorithm was used to classify stem–calyx from true defect areas. The feedforward network structure was suitable for handling nonlinear relationships between input and output variables of prediction-

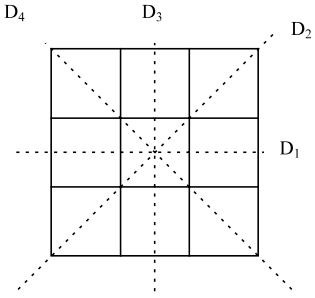

Fig. 4. Four oriented fractal dimensions.

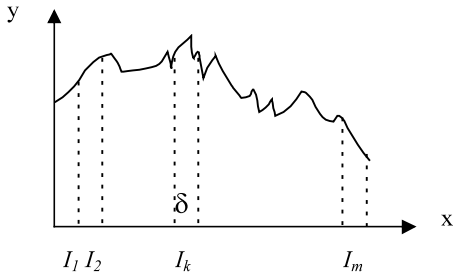

Fig. 5. Oriented fractal curve.

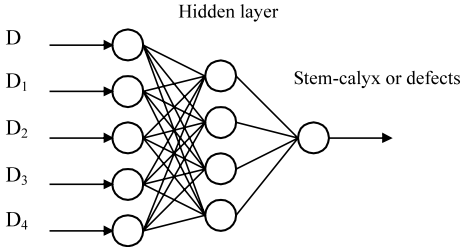

Fig. 6. Network for classify stem–calyx from defects.

related problems. The designed BP network is shown in Fig. 6. The NN model had five input nodes, one hidden layer with four hidden nodes, and one output node. During the training process, the weights of the network were updated after each pass through all the training samples. The convergence of the learning was judged by two conditions: whether the mean squared error for all training samples were smaller than a tolerance value. and whether the output errors for each training sample were smaller than another predefined tolerance value

3.4. Real-time implementation of apple surface defect detection

The real-time implementation of apple surface defect detection is divided into two stages. The first is the segmentation of doubtful spot areas, including defects and stem–calyx areas, by the method described in Section 3.2. The segmentation results show that the stem–calyx areas are often with bigger areas. So in the second stage, the segmented spots with areas bigger than a given value are further processed for distinguishing stem–calyx concave areas from defects by the method presented in Section 3.3.

4. Tests and results

The algorithm was used to detect defects and stem–calyx areas in forty samples of Fuji apples. Some results are shown in Fig. 7, where (a), (c), (e), and (g) are the

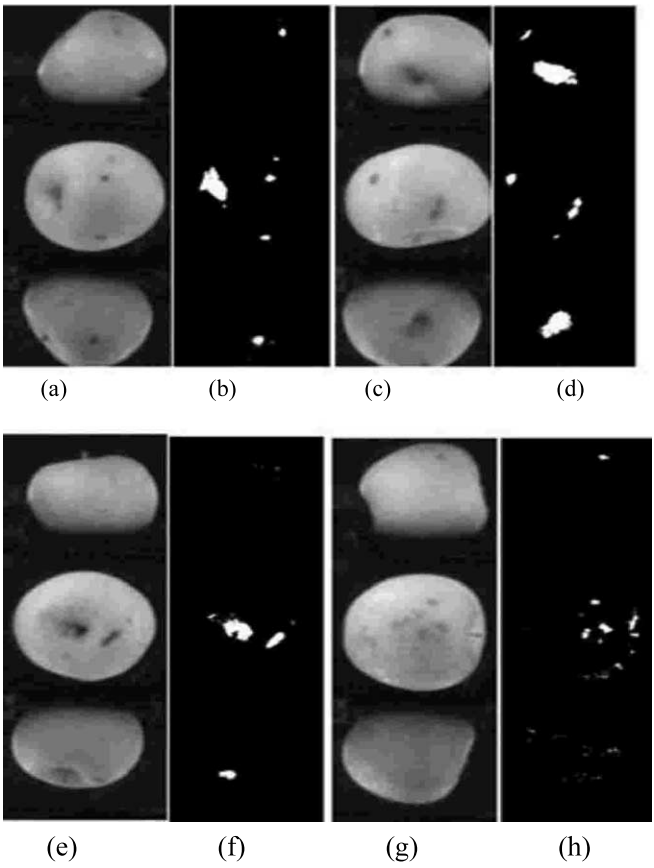

Fig. 7. Defects segmentation results. (a), (c), (e), (g) Original image; (b), (c), (f), (h) segmented defects.

original image of the apples to be inspected, and (b), (d), (f), and (h) are the defect segmentation results. These results show that the defects and stem–calyx areas were basically extracted. The segmented spots with area bigger than a given value were further processed for distinguishing stem–calyx concave area from defects by the method in Section 3.3. Table 1 lists some results of the stem–calyx recognition by the BP network. If the output value of the network is near 1, the detected patch is the stem–calyx area. Similarly, if the output value is near 0, the detected patch is a true defect area. The test results show that the accuracy of the network classifier was over 93%. The Number 16 and 23 defect patches in Table 1 were rotten areas and the degree of rot was so high that their surfaces were concave. The results show that the input fractal features are effective for classifying concave surfaces from normal fruit surfaces. Because the stem–calyx patches are usually concave in shape, the proposed method for stem–calyx recognition is feasible. The processing time for the defect detection and grading for one apple was 320 ms with microcomputer (processor speed: 500 MHz).

Table 1
Some test results of the stem–calyx recognition BP network

Serial number	Input patches	Output of network
1	Stem–calyx: 31 × 31	0.9854
2	Stem–calyx: 38 × 38	0.9949
3	Stem–calyx: 32 × 32	0.6393
4	Stem–calyx: 37 × 37	0.9854
5	Stem–calyx: 39 × 39	0.9526
6	Stem–calyx: 40 × 40	0.9783
7	Stem–calyx: 44 × 44	0.8639
8	Stem–calyx: 44 × 44	0.9840
9	Stem–calyx: 44 × 44	0.8314
10	Stem–calyx: 46 × 46	0.9725
11	Stem–calyx: 48 × 48	0.8874
12	Stem–calyx: 48 × 48	0.9314
13	Stem–calyx: 43 × 43	0.9956
14	Stem–calyx: 47 × 47	0.9434
15	Stem–calyx: 47 × 47	0.8373
16	Defect: 42 × 42	0.9948
17	Defect: 49 × 49	0.0593
18	Defect: 54 × 54	0.0365
19	Defect: 61 × 61	0.0539
20	Defect: 62 × 62	0.2743
21	Defect: 81 × 81	0.2659
22	Defect: 48 × 48	0.0994
23	Defect: 55 × 55	0.8194
24	Defect: 54 × 54	0.0312
26	Defect: 63 × 63	0.0883
27	Defect: 66 × 66	0.2093
28	Defect: 51 × 51	0.2150
29	Defect: 62 × 62	0.0743
30	Defect: 84 × 84	0.2016

5. Conclusions

The results show that the input fractal features are effective for classifying concave surfaces from the normal fruit surfaces. Because the stem–calyx particles are usually concave in shape the proposed method for stem–calyx recognition is feasible.

The system has the advantage of being able to inspect, simultaneously, four aspects of each apple on a sorting line. Furthermore, based on the reference image of an apple, the developed method of defect segmentation can extract most of the surface defects on apples at a speed commensurate with the requirements of a practical grading system, which is the objective of further research.

Acknowledgements

It is gratefully acknowledged that this work is supported under University Doctoral Course Special Fund (Project No. 950801).

References

Growe, T.G., Delwiche, M.J., 1996. Real-time defect detection in fruit—part I: design concepts and development of prototype hardware. Trans. ASAE 39 (6), 2299–2308.

Li, Q., Wang, M., 1999. Study on high-speed apple surface defect segment algorithm based on computer vision. Proceedings of International Conference on Agricultural Engineering (99-ICAE), Beijing, People's Republic of China, 14-17 December 1999, pp. V27–31.

Li, Q., Wang, M., 2000. A fast identification method for fruit surface defect based on fractal characters. J. Image Graphics (China) 5 (2), 144–148.

Tao, Y., 1996. Spherical transform of fruit images for on-line defect extraction of mass objects. Opt. Eng. 35 (2), 344–350.

Throop, J.A., Aneshansley, D.J., Upchurch, B.L., 1997. Apple orientation on automatic sorting equipment. Proceedings of the Sensors for Nondestructive Testing International Conference, NRAES, Ithaca, NY, pp. 328–342.

Yang, Q., 1993. Finding stalk and calyx of apples using structured lighting. Comput. Electron. Agric. 8, 31–42.

Wen, Z., Tao, Y., 1998. Method of dual-camera NIR/MIR image for fruit sorting. ASAE paper 983043. St. Joseph, MI.